ELSEVIER

Contents lists available at ScienceDirect

Journal of Magnetism and Magnetic Materials

journal homepage: www.elsevier.com/locate/jmmm



Hydrothermal synthesis, structural analysis and room-temperature ferromagnetism of Y₂O₃:Co²⁺ nanorods



Prasanta Dhak, Sandeep K.S. Patel, Min-Kwan Kim, Jae-Hyeok Lee, Miyoung Kim, Sang-Koog Kim*

National Creative Research Initiative Center for Spin Dynamics and Spin-Wave Devices, and Research Institute of Advanced Materials, Department of Materials Science and Engineering, Seoul National University, Seoul 151 – 744, Republic of Korea

ARTICLE INFO

Article history:
Received 7 December 2015
Received in revised form
1 February 2016
Accepted 7 February 2016
Available online 8 February 2016

Keywords: Hydrothermal synthesis Y_2O_3 nanorods Room temperature ferromagnetism

ABSTRACT

 Co^{2+} -doped Y_2O_3 nanorods of 70–100 nm diameters and 0.3–2 μ m lengths with different compositions (x=0.00, 0.04, 0.08) in $Y_{2-x}Co_xO_3$ were synthesized by an easy hydrothermal method. The X-ray diffraction, Raman spectra, X-ray photoelectron spectroscopy and transmission electron microscopy (TEM) results indicated the formation of a pure cubic phase structure of Y_2O_3 doped with Co^{2+} ions without any secondary phase formation. The TEM analysis indicated that the nanorods were grown along the [100] axis. The pure Y_2O_3 nanorods showed diamagnetism whereas the Co^{2+} -doped ones exhibited room-temperature ferromagnetism. The existence of such room-temperature ferromagnetic behavior in Co^{2+} -doped Y_2O_3 nanorods is due mainly to the existence of oxygen vacancies originating after the doping of transition metal ions in the Y_2O_3 host lattice. Oxygen vacancies act as defect centers in the bound magnetic polaron model to account for this dilute magnetic oxide of medium band gap with low transition-metal-ion concentration. The presence of defect-related oxygen vacancies was further confirmed by photoluminescence spectra analysis of our studied materials.

© 2016 Elsevier B.V. All rights reserved.

1. Introduction

In recent research, dilute magnetic oxide (DMO) systems are one of the promising candidates for potential spintronics application, because they display room-temperature ferromagnetism [1]. The development of spintronics research has provided many revolutionary possibilities for semiconductor technology [2]. The recent literature on transition-metal-ion-doped room-temperature ferromagnetism in low-band-gap (~3.0 eV) ZnO, TiO₂, SnO₂ and In₂O₃ systems is vast [3–8]. Although the origin of such roomtemperature ferromagnetism in these oxides is explained by the bound magnetic polaron (BMP) model [9-10], there remains controversy with respect to its scientific explanation. There have been few reports of the existence of ferromagnetism in Cr-doped In₂O₃ [8], whereas it has been established that Fe-doped TiO₂ exhibits paramagnetism [7]. Griffin [11] and Tian at al. [12] have reported non-intrinsic ferromagnetism due to the formation of ferromagnetic clusters or impurity. According to the BMP model, oxygen vacancies play an important role in determining the existence of ferromagnetism in such DMOs. Because the oxygenvacancy concentration (V_0) can be controlled, the saturation magnetization can be modulated accordingly [9,13].

Meanwhile, for hybrid device application in the present research, high-κ dielectric systems such as Y₂O₃ are of great interest. Recently, a number of researchers have reported the existence of room-temperature ferromagnetism in transition-metal-ion-doped Y_2O_3 thin films and nanocrystals [14–16], though little attention has been paid to one-dimension (1D) nanostructures. Studies on 1D semiconductor nanostructures have generated huge interest in the last decade, owing to the extraordinary lengths, flexibility, shape anisotropy and unique electronic features due to the 1D quantum confinement effect [17-19]. Thus, we have focused our research on the DMO doped with transition metal ions. In the present study, we synthesized $Y_{2-x}Co_xO_3$; (x=0.00, 0.04, 0.08) nanorods by a cheap and easy hydrothermal method and studied the room-temperature magnetic properties of pure and transitionmetal-ion Co^{2+} -doped Y_2O_3 nanorods. The hydrothermal method was used in the preparation of the 1D nanostructure, because it requires neither templates nor catalysts to yield the product continuously. The details of the synthesis mechanism, a structural and microstructural analysis along with an explanation for the existence of room-temperature ferromagnetism in the Co²⁺-doped Y_2O_3 nanorods are provided. The combination of ferromagnetism with the high- κ dielectric characteristics of the Co²⁺-ion-doped Y₂O₃ will facilitate the integration of complementary metal-oxide semiconductors with spintronics technology.

^{*} Corresponding author. E-mail address: sangkoog@snu.ac.kr (S.-K. Kim).

2. Experimental

Typical synthesis of pure and Co²⁺-doped Y₂O₃ nanorods was carried out via a controlled hydrothermal reaction method. In the preparation of the $Y_{2-x}Co_xO_3$; [x=0.00, 0.04 and 0.08] nanorods, Y₂O₃ was first dissolved in HCl to form a soluble precursor solution, followed by addition of stoichiometric amounts of CoCl₂.6H₂O solution as per the requirements of the compositions. Then, an appropriate amount of NH₄OH solution was slowly added to obtain the hydroxide precipitate of the metal ions, and the final pH of the solution was maintained at \sim 11 to 12. The whole solution was then vigorously stirred for 20 min to ensure thorough mixing. Next, the resultant white slurry was transferred into a stainless steel Teflon-lined autoclave, and solvothermal treatment entailing heating of the autoclave in an oven at 190 °C for 20 h was performed. The final solid product was filtered, washed with water several times, and then dried in vacuum at room temperature. The dried product was then calcined at 600 °C for 4 h to remove any organic contaminants.

The size and morphology of our samples were observed under a transmission electron microscope (TEM, Hitachi H-8100) with an acceleration voltage of 200 kV and a scanning electron microscope (SEM, JEOL, JSM 840A). The phase purity and crystallinity were examined using a PANalytical X'Pert Pro X-ray diffractometer (XRD) with a Cu K α target (λ =1.5418 Å) in a wide range of Bragg angles 2θ ($10^{\circ} \le 2\theta \le 70^{\circ}$) at a scanning rate of $2^{\circ}(2\theta)/\min$. For further detailed structural analysis, Raman spectroscopy measurements were performed using a micro-Raman spectrometer (Model HORIBA Jobin Yvon, $\lambda = 514$ nm line of laser as the excitation source). Further, to obtain information on the elemental composition, the binding energies and oxidation states of the Y, O, and Co elements present in the pure Y₂O₃ and Co-doped Y₂O₃ samples, X-ray Photoelectron spectroscopy (XPS) was carried out using the Thermo Fisher Scientific Multilab 2000 (England) device with Al K α radiation (1486.6 eV). The magnetic properties were studied with a Quantum Design MPMS SQUID. Photoluminescence (PL) measurements were performed on a fluorescence spectrophotometer (LS-55, Perkin Elmer) at room temperature with a wavelength of 390 nm as the excitation source.

3. Results and discussion

The surface morphology was examined by SEM. Fig. 1(a-c) demonstrate the straight rod-shape morphology of the pure and Co-doped Y_2O_3 samples of 70–100 nm average diameter and 0.3–2 μ m length. The images show that the synthesized nanorods had a highly dense nanostructure with an almost uniform size distribution. From the SEM observations, it was revealed that the individual nanorods possess uniform diameters throughout their lengths, with an average aspect ratio generally greater than 20. Although Co-doped Y_2O_3 formed with increasing Co^{2+} doping

concentration, the size of the nanorods slightly decreased. This reflected the fact that the grain growth of the nanorods was somewhat suppressed with the incorporation of dopant into the host lattice, which result might be related to higher stacking fault density [20].

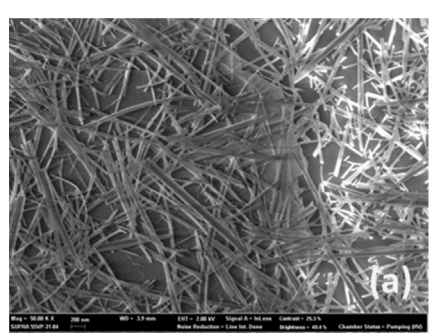
For detailed morphological and structural study, TEM and HRTEM micrographs of our samples were recorded. Fig. 2(a) shows the rod-shaped morphology with the $\sim\!100$ nm average diameter and 2 μm length. As shown in Fig. 2(b), well-defined lattice fringes are observable, and the distance between the crystal planes were measured to 0.3 nm, which corresponds to the (222) crystal plane of cubic Y_2O_3 nanorods according to the values reported in the JCPDS card number 41-1105; this result, moreover, is in agreement with the corresponding electron diffraction pattern [21]. The SAED pattern of the nanorods in Fig. 2(c) exhibits diffraction spots corresponding to the (211), (222) and (400) lattice planes of cubic-phase Y_2O_3 . The elemental mapping images in Fig. 2(d), meanwhile, indicate a homogeneous distribution of Y, O and Co in the $Y_{1.96}Co_{0.04}O_3$ nanorod.

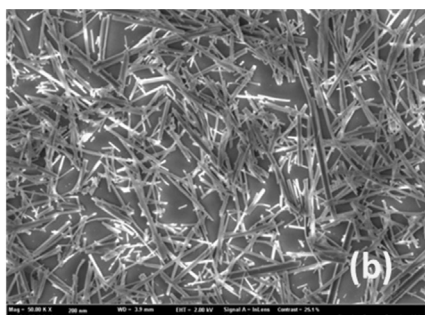
A probable mechanism of nanorod formation is as follows. During the synthesis of $Y_{2-x}Co_xO_3$ nanorods, the pH of the precursor solution was maintained at around 11-12. The yttrium source primarily was in the form of $Y(OH)_3$ precipitates. Portions of these $Y(OH)_3$ precipitates were decomposed during the reaction process, thus forming a large number of Y_2O_3 nuclei. A certain number of these precipitates were transformed into $[Y(OH)_6]^{3-}$ growth units under the highly alkaline conditions. The Y_2O_3 nuclei served here as seeds for the polar growth of Y_2O_3 crystal along the [100] axis through the adsorption of growth units $[Y(OH)_6]^{3-}$ [22]. The probable reaction process for nanorod formation is as follows:

 $Y(OH)_3 + [Y(OH)_6]^{3-} \rightarrow Y(OH)_3 + [Y(OH)_6]^{3-}$ (crystal seeds) \rightarrow aggregation of crystal seeds $\rightarrow Y(OH)_3 + [Y(OH)_6]^3$ (solid spheres) \rightarrow growth in the [001] axis $\rightarrow Y(OH)_3 + [Y(OH)_6]^{3-}$ (nanorods) \rightarrow annealing $\rightarrow Y_2O_3/Y_2O_3$:Co²⁺ nanorods.

It is well known that, in face-centered cubic-structure particles, there are three faces, namely (111), (110) and (100), that differ in their surface atom densities, electronic structure, bonding, and chemical reactivates; accordingly, the surface free energies of the crystallographic planes are in the ascending order $\gamma(111) < \gamma(110) < \gamma(100)$ [23]. It is therefore obvious that the activation energy will be lowered and the bonding ability and chemical reactivity will be higher for the (100) facet than for the other two. Accordingly, the Y_2O_3 crystal will grow preferably in the (100) direction and form rod-shape nanocrystals.

Next, the phase of the calcined powders of the $Y_{2-x}Co_xO_3$; [x=0.00, 0.04, 0.08] nanorods was identified by careful analysis of the XRD Rietveld refinement of the diffraction data using the Fullprof program, as shown in Fig. 3. All of the XRD peaks were identified and indexed according to the JCPDS (card number 41-1105). The Rietveld refinement parameters of the $Y_{2-x}Co_xO_3$; [x=0.00, 0.04, 0.08] nanorods are listed in Table 1. The XRD patterns properly matched the pure-phase cubic crystal structure and





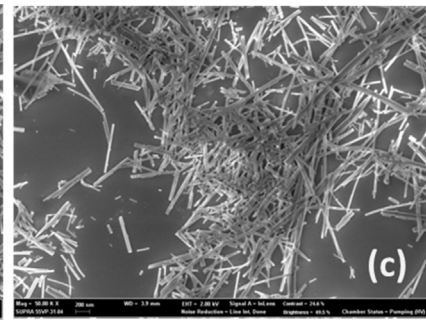


Fig. 1. FESEM images of $Y_{2-x}Co_xO_3$; (a) x=0.00, (b) x=0.04, and (c) x=0.08 nanorods annealed at 600 °C for 4 h.

Download English Version:

https://daneshyari.com/en/article/1798212

Download Persian Version:

https://daneshyari.com/article/1798212

Daneshyari.com